Gas phase chemistry of the heterocumulene cations O=C=N⁺=C=O and O=C=C=N⁺=O

Márcia C. Carvalho, Valmir F. Juliano, Concetta Kascheres * and Marcos N. Eberlin *

State University of Campinas-UNICAMP, Institute of Chemistry CP 6154 13083–970 Campinas, SP, Brazil

The low energy collisional dissociation and ion/molecule chemistry of the heterocumulene cations O=C=N⁺=C=O **1** and O=C=C=N⁺=O **2** have been investigated by pentaquadrupole mass spectrometry, and G2(MP2) *ab initio* calculations applied to interrogate their relative stabilities and dissociation thresholds, as well as those of six other conceivable $C_2NO_2^+$ isomers **3–8**. The calculations show that the acyclic **1** (zero) and **2** (72.4 kcal mol⁻¹) are the most stable isomers, whereas both the location of the positive charge mainly at the CO-carbon and the short CO bond lengths characterize their acylium ion structures. Two cyclic isomers, *i.e.* **7** (131.3 kcal mol⁻¹) and **8** (140.0) kcal mol⁻¹, were also found to be stable, but placed at energy levels considerably higher than **1**. Exactly as predicted from G2(MP2) energy dissociation thresholds, low-energy collisions cause dissociation of **1** exclusively by CO loss to yield NCO⁺ of *m/z* 42. A more diverse dissociation chemistry is predicted and exhibited by **2**, which dissociates mainly by loss of an oxygen atom (C_2NO^+ of *m/z* 54), CO (CNO⁺ of *m/z* 42) and C_2O (NO⁺ of *m/z* 30). Both ions are unreactive towards polar [4+2⁺] cycloaddition with isoprene. However, they undergo ketalization with 2-methoxyethanol, and transacetalization with two cyclic neutral acetals, *i.e.* 2-methyl-1,3-dioxolane and 1,3-dioxane, and these structurally diagnostic ion/molecule reactions confirm experimentally the acylium ion structures of **1** and **2**. Cyclic 'ionic ketals', *i.e.* 1,3-dioxonium ions, are formed in these reactions, as evidenced by their MS³ spectra, which show extensive dissociation to re-form the reactant ions. Whereas **1** readily forms a stable and covalently bound adduct with pyridine, **2** reacts mainly by net CN⁺ and OCN⁺ transfer *via*—most likely—the unstable (Py–**2**)⁺ adduct.

Introduction

Multiple stage mass spectrometry (MSⁿ)[1] offers a variety of techniques by which gaseous ions can be formed and further isolated through mass selection for structural characterization and for the study of their intrinsic physical and chemical properties. Techniques based on dissociative collisions, in particular collision-induced dissociation (CID)[2] and other related techniques such as metastable ion MS (MIKES),[3] energy-resolved MS (ERMS)[4] and neutralization-reionization MS (NRMS)[5] provide a basis in mass spectrometry for the structural characterization of ions. Reactive collisions, *i.e.* ion/molecule reactions,[6] have been less frequently used for ion characterization,[7] but recent examples[8] have shown the power of this technique not only to structurally characterize specific ions of certain structures, but to serve as diagnostic tests for the complete class of structurally related ions. Additionally, gas phase ion/molecule reactions have been able to yield a wealth of information on the intrinsic kinetics, thermochemistry and chemical reactivity of a variety of ionic species of interest.[9]

Schwarz *et al.*[10] recently applied high-energy CID, NRMS and charge-reverse MS for the structural characterization of two heterocumulene cations of $C_2NO_2^+$ composition, *i.e.* **1** and **2**, as well as isomer **3** (see structures below). Ions **1** and **2**, which are isoelectronic with carbon suboxide (O=C=C=C=O), were obtained by dissociative ionization of appropriate precursors and found to be readily distinguishable by high-energy CID and NRMS. The CID spectra of **1** and **2** exhibit peaks of common *m/z* values, mainly those corresponding to ions of C_2NO^+ (*m/z* 54), CNO⁺ (*m/z* 42), C_2O^+ (*m/z* 40), NO⁺ (*m/z* 30) and CO⁺ (*m/z* 28) composition. Ion **2** is characterized, however, by the greater relative abundance of the structurally diagnostic fragments C_2O^+ and NO⁺. The NR mass spectra of **1** and **2** also serve for their structural characterization by showing practically the same set of structurally diagnostic fragments observed in the CID spectra, whereas the recovery signal of *m/z* 70 was

only obtained for **1**. Ion **3** was generated by charge reversal of its stable anion counterpart, and was characterized by a CR mass spectrum that displays a unique, and structurally diagnostic peak, of *m/z* 44 (CO₂⁺).

In spite of the success of high energy CID and NRMS, it would be desirable to have access to other means besides high-energy collision processes for the structural characterization of **1** and **2**. In addition, now that the interesting pair of isomeric heterocumulene cations **1** and **2** has been demonstrated to be readily available species in the gas phase, their chemistry could be explored by multiple stage MS. In this way, and considering that **1** and **2** could be alternatively represented as their resonance hybrids OCN–C⁺=O and ONC–C⁺=O, they could display chemical properties characteristic of acylium ions. This important class of ionic species have recently been found to exhibit a rich chemistry in the gas phase, which includes polar [4+2⁺] cycloaddition with conjugated dienes,[11] ketalization with diols and analogues[12] and transacetalization with neutral cyclic acetals and ketals.[13] Ion **1** has also been found to form abundant stable adducts and loosely-bound dimers in reactions with pyridine,[14] a reactivity that permitted the elaboration of a scale of OCNCO⁺ affinities upon the application of the kinetic method.[15] In the present study, pentaquadrupole (QqQqQ) mass spectrometry[16] is applied to investigate the low energy collision dissociation chemistry and the ion/molecule chemistry of **1** and **2** in the gas phase. The ability of **1** and **2** to undergo reactions that are characteristic of acylium ions has therefore been investigated. Additionally, *ab initio* calculations using the high accuracy GAUSSIAN-2(MP2) model [G2(MP2)][17] have been performed to interrogate the intrinsic stabilities of **1** and **2** in the gas phase, as well as those of the other six conceivable ions of $C_2NO_2^+$ composition **3–8**. With respect to **3** (most likely **7**, see the *ab initio* section), its low-energy collision chemistry could not be investigated since no other means for its gas phase generation other than CRMS[10] appears to be available at the moment.

Table 1 Total energies from G2(MP2) *ab initio* full structural optimization

Species[a]	Electronic state[b]	G2(MP2) Energy (hartree)
1 (rectilinear)	singlet	−280.689 25
1′ (angular)	singlet	−280.693 32
2	singlet	−280.577 49
7	singlet	−280.484 02
8	singlet	−280.470 28
CO	singlet	−113.175 41
NCO⁺	triplet	−167.346 40
O	triplet	−74.978 67
OCNC⁺	singlet	−205.458 96
CNO⁺	triplet	−167.251 07
CCNO⁺	singlet	−205.298 89
OCCN⁺	singlet	−205.473 85
NO⁺	singlet	−129.396 35
C₂O	triplet	−151.038 58

[a] Species **3–6** were found to be unstable, see text. [b] Most stable multiplicity as indicated by the G2(MP2) singlet and triplet energies.

Methods

The MS² and MS³ experiments were performed using an Extrel (Pittsburgh, PA) pentaquadrupole (QqQqQ) mass spectrometer, which has been described in detail elsewhere.[18] Pentaquadrupole mass spectrometers, which are composed basically of a sequential arrangement of three mass analysing (Q1, Q3, Q5) and two 'rf-only' reaction quadrupoles (q2, q4), constitute most suitable 'laboratories' for gas phase ion/molecule reaction studies, a subject that has been reviewed recently.[16] Ion/molecule reactions were performed in the pentaquadrupole by MS² experiments in which Q1 was used to mass select the ion of interest. Reactions were then performed in q2 with a selected neutral reagent at near zero eV collision energies, and at neutral reagent pressures adjusted to maximize reaction yields. The spectrum was acquired by scanning Q5, while Q3 was operated in the 'full-transmission' rf-only mode.

For the MS³ experiments,[19] an ion/molecule reaction product of interest was mass-selected by Q3 and further dissociated in q4 by 15 eV collisions with argon. The total pressures inside each differentially pumped region were typically 2×10^{-6} (ion-source), 8×10^{-5} (q2) and 8×10^{-5} (q4) torr, respectively. The collision energies were calculated as the voltage difference between the ion source and the collision quadrupoles. High resolution measurements were performed on an Autospec mass spectrometer (Micromass-UK) of EBE configuration.

Ab initio molecular orbital calculations were carried out by using GAUSSIAN94.[20] The high accuracy G2(MP2) model[17] was applied in all calculations.

Results and discussion

Which stable C₂NO₂⁺ ions? G2(MP2) *ab initio* calculations

A total of eight isomeric structures, two linear (**1** and **2**), two branched (**3** and **4**) and four cyclic (**5–8**) were considered as chemically reasonable for C₂NO₂⁺ ions. Note that **1/5**, **2/6**, **3/7** and **4/8** are pairs of related cyclic and acyclic isomers. G2(MP2) *ab initio* calculations (see Table 1 and Fig. 1) applied to these eight alternatives indicate that the two linear (**1** and **2**) and two cyclic structures (**7** and **8**) do indeed represent stable gas phase species. Ion **1** is found to be by far the most stable C₂NO₂⁺ isomer, whereas **2**, the second most stable isomer, is placed considerably higher in energy, *i.e.* 72.7 kcal mol⁻¹ above **1**. The cyclic **7** and **8**, although also predicted by the calculations to be stable, are much more energetic species, being placed 131.2 and 140.0 kcal mol⁻¹ above **1**, respectively (Fig. 1).

Structures **3–6** are not predicted to represent stable species at the G2(MP2) level. They do not lie in potential wells, but isomerize to other stable structures without any appreciable
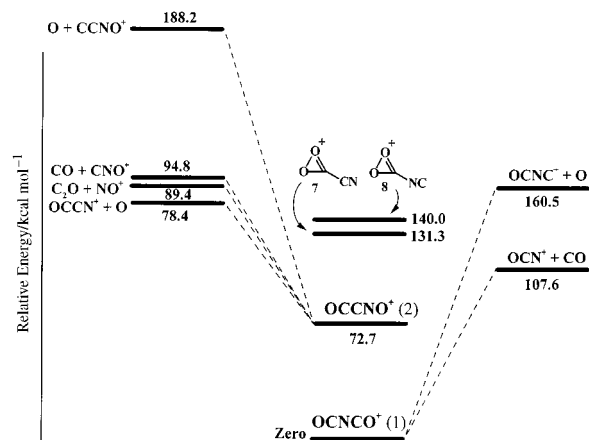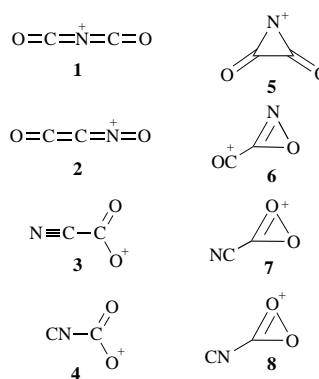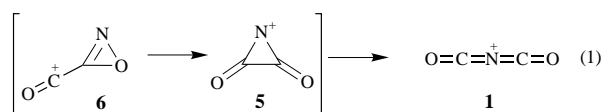
Fig. 1 Relative energies (kcal mol⁻¹) of the four stable C₂NO₂⁺ isomers, and some of their dissociation thresholds, which are given relative to the energies of the precursor ions

energy barrier during the structure optimization procedure. Structures **3** and **4** underwent ring-closure to **7** and **8**, respectively. Ion **5**, an intrinsically unstable nitrenium ion, ring-opened to **1** by C–C cleavage. A quite interesting isomerization process was observed to take place in attempts to optimize the structure of the unstable cyclic ion **6**. Its N–O ring-opening followed by skeletal reorganization yields **1** *via* **5** [eqn (1)].

Also noteworthy was the finding that two energy minimum structures exist for the most stable C₂NO₂⁺ ion **1**. An angular form **1′** (Fig. 2) represents the global minimum, whereas the other stable form is rectilinear **1** and more energetic by only 2.6 kcal mol⁻¹ at the G2(MP2) level. Considering the small energy gap between the two local minimum structures, there might exist an interesting 'flapping' motion that rapidly interconverts both the rectilinear and angular forms of gaseous **1**. The main bond lengths, bond angles and Mülliken charge distribution of **1** and **1′** as well as those of the isomeric **2** are shown in Fig. 2. Note that for both ions the positive charge is mainly located at the CO carbon, whereas the CO bond lengths are considerably shortened (*ca.* 1.16 Å), which characterizes acylium ion structures. Such an acylium ion character is slightly more pronounced in the angular form **1′**.

The G2(MP2) *ab initio* results therefore show **1** and **2** to be the most stable, and the most likely, C₂NO₂⁺ ions to be experimentally observed. Additionally, the calculations indicate that the positive ion sampled in the charge reverse experiment on the CNCO₂⁻ anion[10] most likely exhibited the cyclic structure **7**, which is generated by rapid cyclization of the nascent (and unstable) ion **3**.
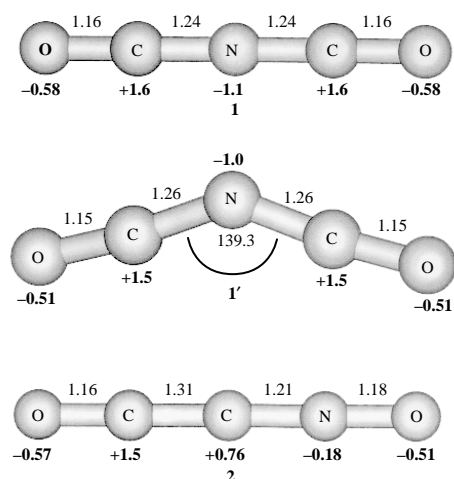
Fig. 2 *Ab initio* MP2/6-31G(d) optimized structures and G2(MP2) Mülliken charge distribution (bold numerals) of the two energy minimum structures of **1**, *i.e.* **1** (rectilinear) and **1′** (angular), and that of the isomeric **2**. Note in both cases the positive charge located mainly on the CO-carbon and the relatively short CO bond length, which characterize acylium ion structures.
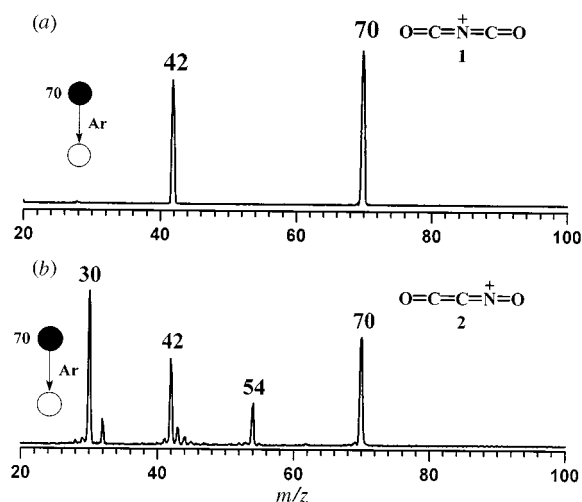

Fig. 3 Double-stage (MS²) low-energy (15 eV) CID product spectrum of (*a*) **1** and (*b*) **2**. Note that **1** dissociates exclusively to *m/z* 42 by CO loss, whereas **2** shows a richer dissociation chemistry that comprises mainly oxygen atom loss (*m/z* 54), CO loss (*m/z* 42) and C₂O loss (*m/z* 30). In the terminology used to describe the type of MSⁿ experiment and scan mode employed, a filled circle ● represents a fixed (or selected) mass; an open circle ○, a variable (or scanned) mass, whereas the neutral reagent or collision gas that causes the mass transitions are shown between the circles. For more details on this terminology, see ref. 19.

Gas phase chemistry of 1 and 2

Dissociative 70 eV EI of ethoxycarbonyl isocyanate and ethylchlorohydroxyiminoacetate were used to generate **1** and **2**, respectively. The latter was the same precursor used by Schwarz *et al.*[10] to form **2**, whereas ethoxycarbonyl isocyanate has been used by Cooks *et al.*[14] to generate **1**. High-resolution measurements on both of these ions of *m/z* 70 reveal a $C_2NO_2^+$ composition greater than 99.9 % [69.9934 (calc. 69.9929)].

Low-energy collisional dissociation chemistry. The CID spectra of **1** and **2** (Fig. 3) were obtained by mass-selecting the ions in Q1 and performing 15 eV collisions with argon in Q2. Note the quite distinct CID low-energy chemistry observed for **1** when compared to that of high-energy CID.[10] Mild collisions promote dissociation of **1** almost exclusively by CO loss that yields NCO⁺ of *m/z* 42 [Fig. 3(a)]. Ion **2**, by contrast, displays considerably similar low- [Fig. 3(b)] and high-energy dissociation chemistry, which also includes CO loss (CNO⁺ of *m/z* 42), and which provides additionally the structurally diagnostic
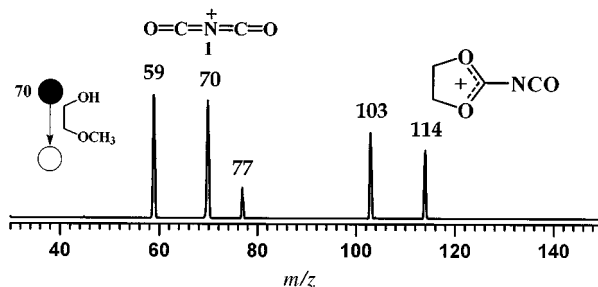

Fig. 4 Double-stage (MS²) product spectrum for reactions of **1** with 2-methoxy ethanol. Note the ketalization product of *m/z* 114, whereas the other products (*m/z* 77, 59, 103) are most likely formed by initial charge-exchange that is followed by proton transfer and subsequent reactions. The product spectrum for **2** is nearly identical to this spectrum and is not shown.

OCCN⁺ (*m/z* 54) and NO⁺ (*m/z* 30) fragments. Also noteworthy is the fact that only **2** loses an oxygen atom (OCCN⁺, *m/z* 54) under low energy collisions, whereas this dissociation pathway is available to both **1** and **2** when high-energy collisions[10] are applied.

To investigate this interesting difference in dissociation behavior, the energy thresholds of several dissociation processes for **1** and **2** were estimated by G2(MP2) *ab initio* calculations. The results are also shown in Table 1, and summarized in Fig. 1. Exactly as experimentally observed for **1**, CO loss is the dissociation process predicted by the calculations to display by far the lowest energy threshold, whereas oxygen atom loss is a much more energy demanding dissociation. For **2**, on the other hand, the inverse situation is observed, and oxygen atom loss from the NO terminal group is the most energetically favourable process. In fact, there is for **2** a 'package' of three dissociation processes that display quite close energy thresholds, *i.e.* those of O, CO and C₂O loss (Fig. 1). Therefore, these three processes are expected to occur predominantly under collision activation, exactly as experimentally observed for **2**. The greater preference of **2** to lose its oxygen atom from the NO terminal group rather than that from CO is therefore a consequence, according to the *ab initio* calculations, of the greater stability of the acylium ion product O=C⁺-CN when compared to that of the alternative C₂NO⁺ fragment ion.

Polar [4+2⁺] cycloadditions.[11] No cycloaddition products are formed when **1** and **2** react with the *s-cis* conjugated diene isoprene (spectra not shown). The main products correspond exactly to the same set of ions (*m/z* 69, 81, 95, 107, 121, 135, 137, 149) obtained in reactions with ionized and protonated isoprene with neutral isoprene.[11a] It is therefore likely that charge exchange is the main primary reaction between **1** and **2** with isoprene. A few acylium ions have been found to be unreactive in [4+2⁺] polar cycloadditons,[11] and therefore it is not a surprise that **1** and **2** are also unreactive.

Ketalization. Recently a number of acylium ions have been shown by pentaquadrupole MS to undergo a novel ketalization reaction with diols and analogues in the gas phase.[12] Cyclic 'ionic ketals', *i.e.* 1,3-dioxonium ions are formed, as evidenced by MS³ and ¹⁸O labelling experiments (the ¹⁸O-labelled cyclic 'ionic ketal' dissociates to both the labelled and unlabelled acylium ion to equal extents), as well as theoretically by *ab initio* calculations.[21] Similar reactions are also observed in reactions of **1** (Fig. 4) and **2** with 2-methoxyethanol, both ions producing nearly identical product spectra. Medium abundant products of *m/z* 114 are formed, which are ascribed to the 2-NCO and 2-CNO cyclic 1,3-dioxolanylium ions, respectively, *i.e.* the cyclic 'ionic ketal' depicted in Scheme 1. The other ionic products are ascribed as following: protonated 2-methoxyethanol of *m/z* 77 MH⁺, (M − OH)⁺ and/or (MH − H₂O)⁺ of *m/z* 59, and [(*m/z* 59) + M − CH₃OH] of *m/z* 103.[22]

Transacetalization. Acylium ions have also been shown
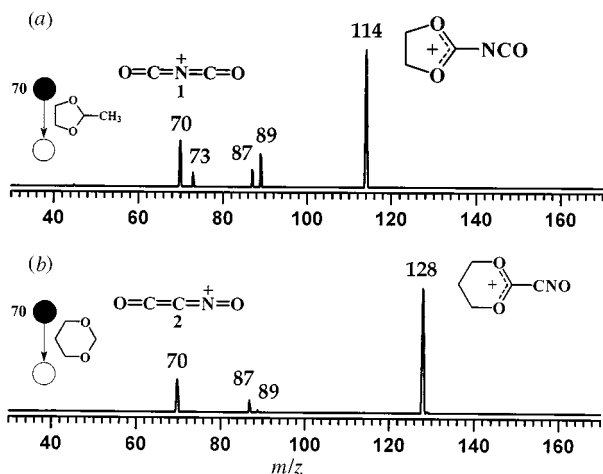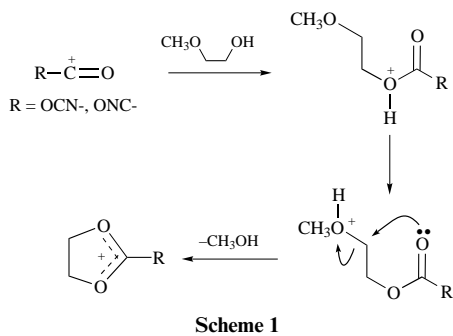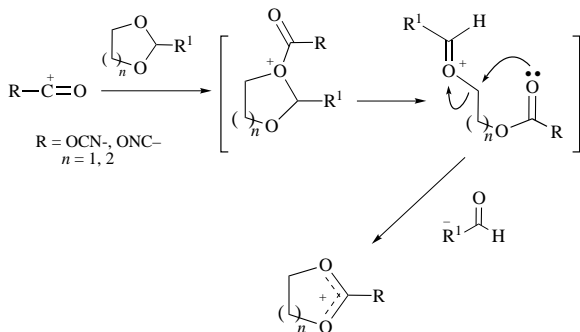
Scheme 1

Fig. 5 Double-stage (MS^2) product spectrum for reactions of (*a*) **1** with 2-methyl-1,3-dioxolane and (*b*) **2** with 1,3-dioxane. Note the abundant transacetalization product, *i.e.* cyclic 'ionic ketals' of *m/z* 114 and 128, respectively.

recently to readily replace carbonyl compounds from cyclic acetals and ketals in novel gas phase transacetalization reactions.[13] The reactions of **1** and **2** with the cyclic acetals 2-methyl-1,3-dioxolane and 1,3-dioxane were then investigated. As exemplified in Fig. 5, transacetalization occurs extensively for both ions, which produce nearly identical product spectra. Abundant ions of *m/z* 114 and 128 are formed, respectively, which are ascribed to the cyclic 'ionic ketal' transacetalization products (Scheme 2). The reaction is likely initiated by *O*-

Scheme 2

acylation (note that initial attack at either oxygen leads to the same final cyclic ion), followed by a ring-opening/ring-closure process that forms the cyclic 'ionic ketal' shown in Scheme 2. This characteristic reactivity has been largely demonstrated to be a very common property, *i.e.* structurally diagnostic for an acylium ion. Thus the acylium ion properties of **1** and **2** are demonstrated by this peculiar reactivity.

Triple-stage mass spectra. Fig. 6 shows the triple-stage (MS^3) mass spectra of the cyclic 'ionic ketals' formed by transacetalization with 2-methyl-1,3-dioxolane and 1,3-dioxane. In both cases, extensive and exclusive dissociation that re-forms the
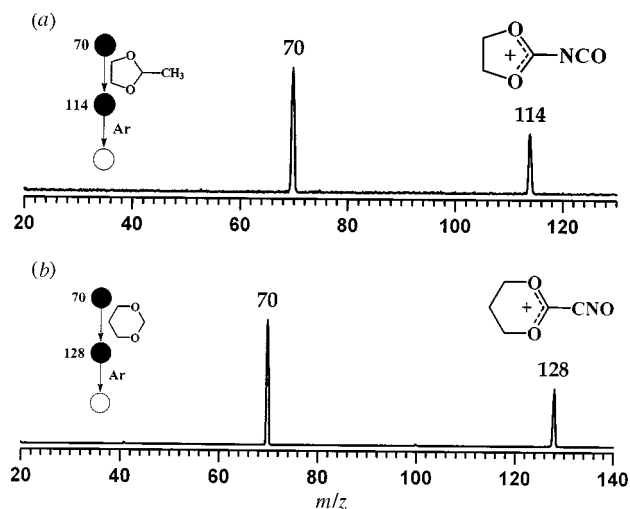
Fig. 6 Triple-stage (MS^3) sequential product spectra of the cyclic 'ionic ketals' formed in reactions of (*a*) **1** with 2-methyl-1,3-dioxolane; and (*b*) **2** with 1,3-dioxane. Note the extensive dissociation to re-form the reactant ion of *m/z* 70 in both cases.
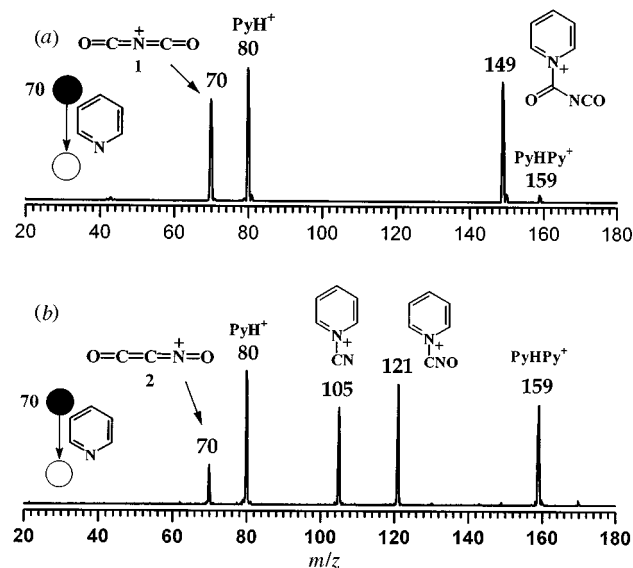
Fig. 7 Double-stage (MS^2) product spectrum for reactions of pyridine with (*a*) **1** and (*b*) **2**. Note that **1** forms an abundant adduct of *m/z* 149, whereas **2** reacts to form most likely an unstable adduct that dissociates rapidly to *m/z* 121 and 105.

reactant ion of *m/z* 70 is observed. Spectra (not shown) nearly identical to that shown in [Fig. 6(*a*)] were obtained for the ketalization products of *m/z* 114 formed in reactions of **1** (Fig. 4) and **2** with 2-methoxyethanol. This unique dissociation chemistry, somewhat analogous to the reforming hydrolysis of neutral acetals and ketals, has been also largely demonstrated to be a peculiarity of cyclic 'ionic ketals'.

Stable and unstable adducts with pyridine. The product spectra for reactions of **1** and **2** with pyridine are shown in Fig. 7. The distinct reactivity of both isomers is remarkable. A very abundant and stable pyridine adduct of *m/z* 149 is formed for **1** [Fig. 7(*a*)], whereas **2** forms apparently an unstable adduct that dissociates rapidly by CO and CO/O or CO$_2$ loss yielding the products Py-CNO$^+$ (*m/z* 121) and Py-CN$^+$ (*m/z* 105), respectively (Scheme 3). The formation of the Py-CNO$^+$ product indicates C-3 as the preferable binding site of **2** to pyridine, as expected if one considers that nucleophilic attack should take place on the carbon next to the positively charged nitrogen. Note that such a diverse reactivity towards pyridine permits straightforward distinction between **1** and **2**.

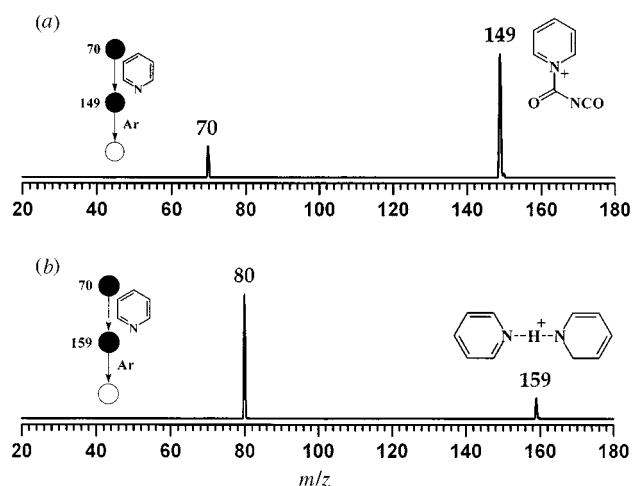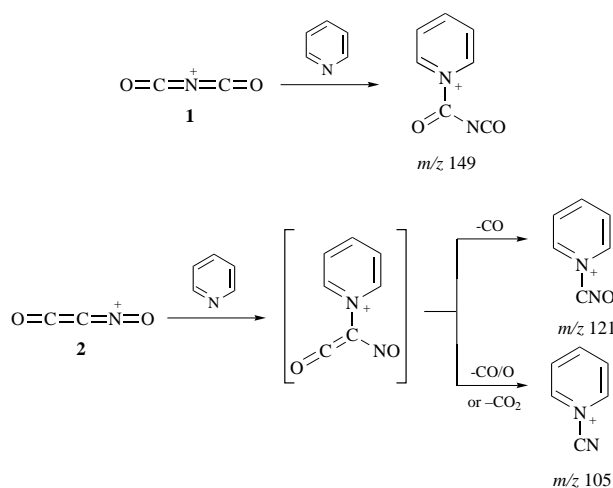The triple-stage spectrum of the putative Py-CNO$^+$ product

Scheme 3

Fig. 8 Triple-stage (MS³) sequential product spectrum of (*a*) the (Py–**1**)⁺ adduct of *m/z* 149 and (*b*) the loosely-bound Py₂H⁺ dimer. Note that under the very same collision conditions, (Py–**1**)⁺ dissociates to a modest extent, whereas extensive dissociation occurs for the loosely-bound Py₂H⁺ dimer.

(not shown) displays two fragments of *m/z* 79 (Py˙⁺, loss of OCN˙) and 52 [(Py − HCN)˙⁺], a dissociation chemistry that is in agreement with its proposed structure. Py-CN⁺, on the other hand, shows high resistance towards collisional dissociation, no fragments being observed in its triple stage spectrum under the low energy collision conditions employed.

The binding nature of the (Py–**1**)⁺ adduct was investigated by recording under very similar conditions its triple stage mass spectrum and that of the loosely-bound proton dimer of pyridine. Such a close comparison was possible in the penta-quadrupole since both ions are formed in reactions of **1** with pyridine [Fig. 7(*a*)] in q2, and they can therefore be sequentially mass-selected by Q3 in the same experimental setup for further collisional dissociation in q4. Under collision conditions that cause extensive dissociation of [Py-H-Py]⁺ [Fig. 8(*a*)], (Py–**1**)⁺ undergoes dissociation to a quite modest extent [Fig. 8(*b*)]. This indicates that the (Py–**1**)⁺ adduct is a covalently bound species.

Conclusions

The heterocumulene cations **1** and **2**, according to the high accuracy G2(MP2) *ab initio* results, are the two most stable C₂NO₂⁺ isomers, being therefore the most likely for experimental observation. They display quite diverse low-energy collision-induced dissociation chemistry and ion/molecule reactivity with pyridine, and are therefore readily distinguished

in the gas phase. The dissociation chemistries of **1** and **2**, which are in perfect agreement with G2(MP2) energy dissociation thresholds, firmly corroborate the structural assignments. Additionally, the similar structurally diagnostic reactivity of **1** and **2** towards ketalization and transacetalization clearly characterize their acylium ion structures.

References

1 K. L. Busch, G. L. Glish and S. A. McLuckey, *Mass Spectrometry/ Mass Spectrometry: Techniques and Applications of Tandem Mass Spectrometry*, VCH, New York, 1988.
2 (*a*) F. W. McLafferty, *Tandem Mass Spectrometry*, Wiley, New York, 1983; (*b*) K. Levsen and H. Schwarz, *Mass Spectrom. Rev.*, 1983, **2**, 77; (*c*) J. L. Holmes, *Org. Mass Spectrom.*, 1985, **20**, 169.
3 R. G. Cooks, J. H. Beynon, R. M. Caprioli and G. R. Lester, *Metastable Ions*, Elsevier, New York, 1973.
4 S. A. McLukey, L. Sallans, R. B. Cody, R. C. Burnier, S. Verma, B. S. Freiser and R. G. Cooks, *Int. J. Mass Spectrom. Ion Phys.*, 1982, **44**, 215.
5 (*a*) C. Wesdemiotis and F. W. McLafferty, *Chem. Rev.*, 1987, **87**, 485; (*b*) H. Schwarz, *Pure Appl. Chem.*, 1989, **61**, 984; (*c*) D. V. Zagorevskii and J. L. Holmes, *Mass Spectrom. Rev.*, 1994, **13**, 133.
6 (*a*) *Ion-Molecule Reactions, Spectrometry*, ed. J. L. Franklin, Plenum Press, New York, 1972; (*b*) *Gas Phase Ion/molecule Reactions*, ed. M. T. Bowers, Vols. 1–3, Academic Press, New York, 1979; (*c*) '*Techniques for the Study of Ion-Molecule Reactions*', eds J. M. Farrar and W. H. Saunders, Wiley, New York, 1988.
7 For some examples, see: (*a*) J. Jalonen, *J. Chem. Soc., Chem. Commun.*, 1985, 872; (*b*) M. T. Kinter and M. M. Bursey, *J. Am. Chem. Soc.*, 1986, **108**, 1797; (*c*) T. G. Heath, J. Allison and J. T. Watson, *J. Am. Soc. Mass Spectrom.*, 1991, **2**, 270; (*d*) B. J. Shay, M. N. Eberlin, R. G. Cooks and C. Wesdemiotis, *J. Am. Soc. Mass Spectrom.*, 1992, **3**, 518; (*e*) A. E. P. M. Sorrilha, F. C. Gozzo, R. S. Pimpim and M. N. Eberlin, *J. Am. Soc. Mass Spectrom.*, 1996, **7**, 1126.
8 (*a*) M. N. Eberlin and R. G. Cooks, *Org. Mass Spectrom.*, 1993, **28**, 679; (*b*) H. I. Kenttämaa and R. G. Cooks, *J. Am. Chem. Soc.*, 1989, **111**, 4122; (*c*) K. K. Thoen, B. J. Beasley, R. L. Smith and H. I. Kenttämaa, *J. Am. Soc. Mass Spectrom.*, 1996, **7**, 1250.
9 See *e.g.*, (*a*) C. Sparapani and M. Speranza, *J. Am. Chem. Soc.*, 1980, **102**, 3120; (*b*) J. K. Kim and M. C. Caserio, *J. Am. Chem. Soc.*, 1982, **104**, 4624; (*c*) T. Kotiaho, B. J. Shay, R. G. Cooks and M. N. Eberlin, *J. Am. Chem. Soc.*, 1993, **115**, 1004; (*d*) S. T. Graul and R. R. Squires, *J. Am. Chem. Soc.*, 1990, **112**, 2517; (*e*) M. N. Eberlin, T. Kotiaho, B. J. Shay, S. S. Yang and R. G. Cooks, *J. Am. Chem. Soc.*, 1994, **116**, 2457; (*f*) C. Beaugrand, D. Jaouen, H. Mestdagh and C. Rolando, *Anal. Chem.*, 1989, **61**, 1447; (*g*) K. Eller and H. Schwarz, *Chem. Rev.*, 1991, **91**, 1121; (*g*) M. N. Eberlin, A. E. P. M. Sorrilha, F. C. Gozzo and R. S. Pimpim, *J. Am. Chem. Soc.*, 1997, **119**, 3550; (*h*) P. S. H. Wong, S. Ma, S. S. Yang, F. C. Gozzo and M. N. Eberlin, *J. Am. Soc. Mass Spectrom.*, 1997, **8**, 68.
10 D. Sülzle, P. E. O′Bannon and H. Schwarz, *Chem. Ber.*, 1992, **125**, 279.
11 (*a*) M. N. Eberlin, T. K. Majumdar and R. G. Cooks, *J. Am. Chem. Soc.*, 1992, **114**, 2884; (*b*) M. N. Eberlin and R. G. Cooks, *J. Am. Chem. Soc.*, 1993, **115**, 9226.
12 L. A. B. Moraes, R. S. Pimpim and M. N. Eberlin, *J. Org. Chem.*, 1996, **61**, 8726.
13 (*a*) P. Vainiotalo, L. A. B. Moraes and M. N. Eberlin, *Proceedings of the 44th ASMS Conference on Mass Spectrometry and Allied Topics*, 1996, p. 453; (*b*) L. A. B. Moraes, F. C. Gozzo, M. N. Eberlin and P. Vainiotalo, *J. Org. Chem.*, 1997, **62**, 5096; (*c*) L. A. B. Moraes and M. N. Eberlin, *J. Chem. Soc., Perkin Trans. 2*, 1997, 2105.
14 S. S. Yang, G. Chen, S. Ma, R. G. Cooks, F. C. Gozzo and M. N. Eberlin, *J. Mass Spectrom.*, 1995, **30**, 807.
15 R. G. Cooks, S. Patrick, T. Kotiaho and S. A. McLuckey, *Mass Spectrom. Rev.*, 1994, **13**, 287.
16 M. N. Eberlin, *Mass Spectrom. Rev.*, in press.
17 The G2 and G2(MP2) methods adopt a composite procedure based

effectively on QCISD-(T)/6-311G+(3df,2p)//MP2(full)/6-31G(d) energies (evaluated by making certain additivity assumptions) together with ZPE and isogyric corrections, and they have been shown to produce results with high accuracy in various chemical systems, see L. A. Curtis, K. Raghavachari and J. A. Pople, *J. Chem. Phys.*, 1993, **98**, 1293.

18 V. F. Juliano, F. C. Gozzo, M. N. Eberlin, C. Kascheres and C. L. Lago, *Anal. Chem.*, 1996, **68**, 1328.
19 J. C. Schwartz, A. P. Wade, C. G. Enke and R. G. Cooks, *Anal. Chem.*, 1990, **62**, 1809.
20 GAUSSIAN 94, Revision B.3, M. J. Frisch, G. W. Trucks, H. B. Schlegel, P. M. W. Gill, B. G. Johnson, M. A. Robb, J. R. Cheeseman, T. Keith, G. A. Petersson, J. A. Montgomery, K. Raghavachari, M. A. Al-Laham, V. G. Zakrzewski, J. V. Ortiz, J. B. Foresman, C. Y. Peng, P. Y. Ayala, W. Chen, M. W. Wong, J. L. Andres, E. S. Replogle, R. Gomperts, R. L. Martin, D. J. Fox, J. S. Binkley, D. J. Defrees, J. Baker, J. P. Stewart, M. Head-Gordon, C. Gonzalez and J. A. Pople, Gaussian, Inc., Pittsburgh PA, 1995.
21 L. A. B. Moraes, R. S. Pimpim and M. N. Eberlin, *J. Org. Chem.*, in the press.
22 J. M. H. Pakarinen and P. Vainiotalo, *J. Mass Spectrom.*, 1996, **31**, 1003.